Modes of remodeling in the cortical cytoskeleton of vascular endothelial cells

Devrim Pesen, Jan H. Hoh*

Department of Physiology, Johns Hopkins University, School of Medicine, 725 N. Wolfe Street, Baltimore, MD 21205, USA

Received 2 November 2004; revised 1 December 2004; accepted 6 December 2004

Available online 18 December 2004

Edited by Amy McGough

Abstract The cortical cytoskeleton of vascular endothelial cells plays an important role in responding to mechanical stimuli and controlling the distribution of cell surface proteins. Here, we have used atomic force microscopy to visualize the dynamics of cortical cytoskeleton in living bovine pulmonary artery endothelial cells. We demonstrate that the cortical cytoskeleton, organized as a complex polygonal mesh, is highly dynamic and shows two modes of remodeling: intact-boundary-mode where mesh element boundaries remain intact but move at ~0.08 μm/min allowing the mesh element to change shape, and altered-boundary-mode where new mesh boundaries form and existing ones disappear.

© 2004 Federation of European Biochemical Societies. Published by Elsevier B.V. All rights reserved.

Keywords: Endothelial cell; Cytoskeletal dynamics; Atomic force microscopy; Mechanotransduction

1. Introduction

Vascular endothelial cells (VECs) play an important role in sensing mechanical changes in the blood stream and signaling surrounding cells and tissues [1,2]. This signaling is thought to depend on cytoskeleton; for example, in the decentralized model the signaling cascade is initiated by mechanical perturbations at the cell surface, which are then propagated to distal parts of the cell via the cytoskeleton [3]. Cortical cytoskeleton, the cytoskeleton in contact with and close proximity to the cell apical plasma membrane, plays two direct roles. To begin with, the cortical cytoskeleton is proximal to the forces exerted by the blood stream and is thus the first cytoskeletal component to be effected by local mechanical changes. Further, the cortical cytoskeleton is a determinant of cell surface shape, which in turn affects the local shear stress distribution [3,4]. The cortical cytoskeleton also plays an important role in the organization of various membrane components on the VEC surface. The location of integrins coupled to the cytoskeleton is determined by the cytoskeletal organization at the cell surface. It has also been proposed that movement of diffusive membrane components is controlled by cortical cytoskeleton. In the so-called anchored picket fence model, movement of membrane components is constrained when cytoplasmic domains are confined by cytoskeletal ''fences'' [5,6].

Electron microscopy provides highly detailed views of the cortical cytoskeleton, often revealing a fine and highly complex mesh-like organization [7,8]. However, optical microscopy of the cortex in living cells is technically difficult and as a result little is known about the dynamics of cortical cytoskeleton [9]. Atomic force microscopy (AFM) offers a new approach to visualizing cytoskeleton in living cells [4,10,11]. The differences in mechanical properties of the cytoskeleton and the cell membrane give rise to different surface deformations and thus contribute to contrast in the images allowing direct visualization of the cytoskeleton near the cell surface [12]. Bovine pulmonary artery endothelial cells (BPAECs) are one model system for studying functionally important aspects of cytoskeleton. These cells are derived from the pulmonary vascular endothelium, where they function as a semi-permeable barrier [13]. In several instances, alterations of barrier permeability are mediated by cytoskeletal rearrangements, and hence cytoskeletal organization in these cells has been studied in some detail [14]. Here, we have used AFM imaging to characterize the dynamics of cortical cytoskeleton of living BPAECs.

2. Materials and methods

2.1. Cell culture

BPAECs, Eagle's MEM and fetal bovine serum were from American Type Culture Collection (Manassas, VA). BPAECs were maintained on petri dishes or gelatin-coated glass coverslips in Eagle's MEM supplemented with 20% fetal bovine serum at 5% CO_2 and 37 °C. The cells were fed every 2–3 days and passaged when confluent. Passages 17–22 were used.

2.2. AFM imaging

AFM imaging was performed with a Multimode or Bioscope AFM equipped with large area scanners (>100 μm × 100 μm), with a Nanoscope IIIa controller (Digital Instruments Inc., Santa Barbara, CA). The Bioscope was mounted on an Olympus inverted optical microscope. For imaging live cells in solution, unsharpened (radius of curvature ~50 nm) silicon nitride cantilevers with nominal force constants of 0.01 or 0.03 N/m were used (Nanoprobes, Digital Instruments). Live cell imaging was performed in fluid contact mode at room temperature and atmospheric CO_2. The imaging buffer was phosphate-buffered saline (Invitrogen Carlsbad, CA) supplemented with 1.2 mmol/l $CaCl_2$, 1.2 mmol/l $MgCl_2$, 5 mmol/l HEPES and 5.5 mmol/l glucose. Imaging parameters were empirically optimized to produce clear images with minimal distortion or damage to the cells. Typically, scan rates were 60–120 μm/s, resulting in image acquisition times of 4–16 min depending on the scan size. BPAECs could be imaged for up to 4 h, during which time the cells remained adherent and high quality images could be collected. With extended imaging the fenestrae between cells began to expand, exposing the substrate. We interpret this as an indicator of cell deterioration in response to the AFM imaging. Further imaging resulted in loss of cells from the surface. Generally, the applied force was

*Corresponding author. Fax: +1 410 614 3797.
E-mail address: jhoh@jhmi.edu (J.H. Hoh).

0014-5793/$22.00 © 2004 Federation of European Biochemical Societies. Published by Elsevier B.V. All rights reserved.
doi:10.1016/j.febslet.2004.12.014

on the order of 1 nN. Data presented here are for cells that have been imaged for less than 2 h; however, cells could typically be imaged for up to 4 h without any apparent damage.

2.3. Image display and data analysis

AFM data were analyzed with Image SXM and SuperMapper, a custom software suite developed with Interactive Data Language (Research Systems Inc, Boulder, CO). The deflection images were processed to optimize brightness and to enhance contrast. Immunofluorescence data were optimized for brightness and contrast using Adobe Photoshop. Correlated areas were determined visually by overlaying AFM deflection images on CFM images and manually varying the transparency of the AFM image.

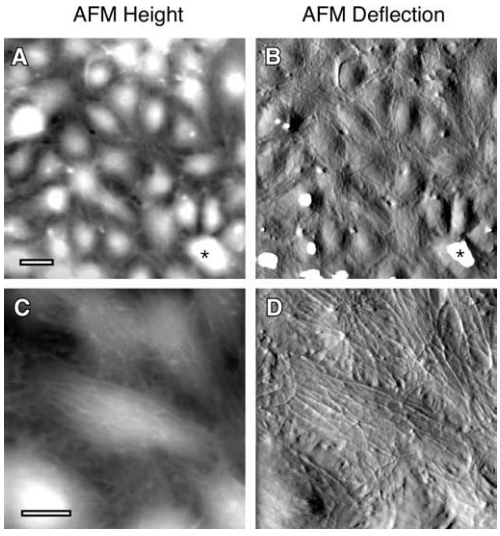

Fig. 1. Organization of cortical cytoskeleton in BPAECs. (A,C) AFM height and (B,D) corresponding deflection images of living BPAECs imaged in physiological saline. (A) and (B) show the typical cobblestone morphology. (D) The deflection image shows an intricate mesh of filaments. The saturated features (asterisk) are imaging artifacts. Z-range of the gray scale in A and C is 0–4 μm (the brighter the higher). The scale bar for A and B is 20 μm; for C and D is 10 μm.

3. Results

AFM images of BPAECs grown in confluent monolayers show cobblestone morphology (Fig. 1). Even though confluent, these monolayers occasionally have small openings exposing the substrate. Measured relative to this substrate the typical cell diameter is tens of micrometers, and cell heights range from a few hundred nanometers at the periphery to ~4 μm towards the center. Furthermore, these cells display a complex cortical filamentous network that is composed in part of actin and vimentin [12]. There is no formal definition of the cell cortex; here we define the cortex as what is accessible to the AFM probe in a typical imaging experiment. Force distance measurements show that the maximal deformation at 1 nN is ~600 nm and examination of the AFM height images suggests that the lower limit for deformation is ~50 nm; thus we estimate the thickness of the cortex to be a few hundred nanometers [12].

Time-lapse imaging of BPAECs shows that the overall position or shape of the cells does not change significantly over several hours, as would be expected for a mature monolayer. However, the cortical cytoskeleton reorganizes itself in a highly dynamic fashion (Fig. 2). Tracing cortical mesh boundaries in sequential images allows us to examine the dynamics of remodeling. We identify two characteristic modes of remodeling for the coarse mesh: intact-boundary-mode (IBM) and altered-boundary-mode (ABM). In IBM, the polygonal mesh elements change size and shape, but the boundaries remain intact. We quantified the IBM remodeling of three mesh elements in one cell during 97 min of imaging (Fig. 3). The rate of movement of several reference points (RPs) in these elements is 0.08 ± 0.01 μm/min ($n = 8$). There was no obvious trend for the change in size and symmetry of mesh elements. The reference points moved in different directions; for instance, RP1 moved up (towards the cell body) and to the right before moving down, while RP2 and RP3 initially moved mostly upwards. RP2 then moved more to the left and RP3 more to the right. Thus, these mesh elements show no directional motion and the overall dynamics of IBM might be de-

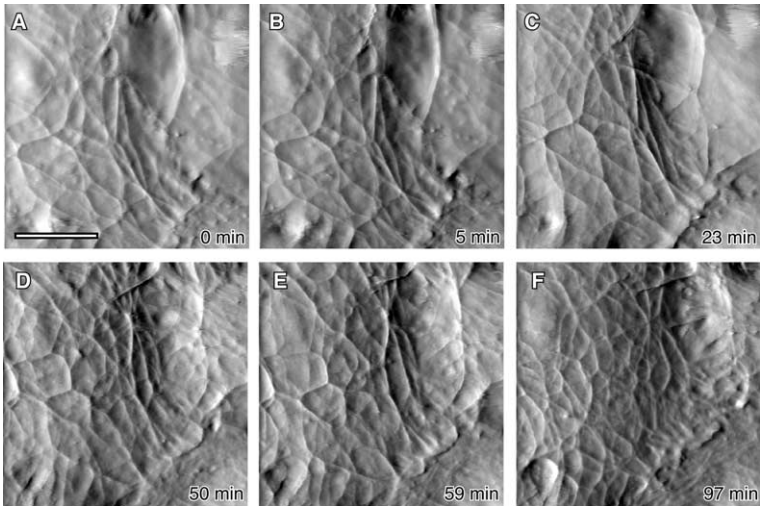

Fig. 2. Time-lapse AFM imaging reveals dynamics of cortical remodeling. (A–F) AFM deflection images of BPAECs in a physiological saline, collected over time, show that the cytoskeletal network is highly dynamic. Comparison of the trace and retrace images show that there are no tip induced lateral distortions of the cytoskeleton under these conditions. Note that because the scan rate is on the order of minutes, events fast relative to this time scale are not captured. Scale bar 10 μm.

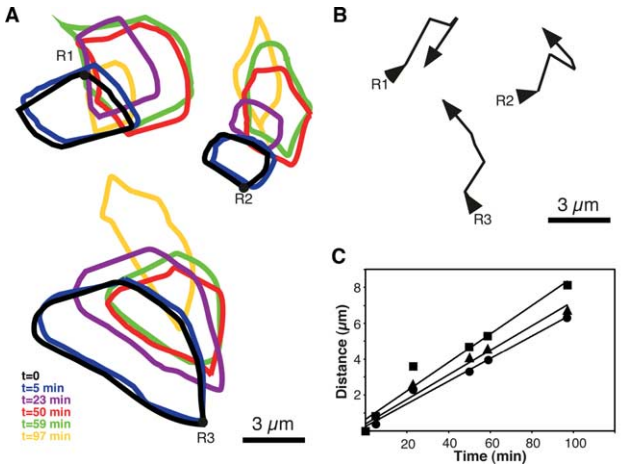

Fig. 3. IBM remodeling of the cortical mesh. Hand traces of coarse mesh boundaries from Fig. 2 that show IBM type remodeling. (A) Mesh elements followed over time change shape and size. (B) Plotting trajectories of reference points on three mesh elements shows that the elements move in slow wiggling fashion. (C) The rate of mesh movement is determined by plotting total distance traveled by each reference point as a function of time. A linear fit to the data gives a rate of 0.08 ± 0.01 μm/min (n = 8).

scribed as a cytoskeletal "wiggle" similar to that described for the vimentin dynamics in endothelial cells under static conditions [15].

In ABM remodeling, filaments and cytoskeletal focal points appeared or disappeared with time, dissolving existing mesh elements and forming elements with new boundaries (Fig. 4). For ABM, it was not possible to track mesh elements before they appeared at the cortex or after they disappeared. Some ABM remodeling occurred between sequential frames and was thus occurring on a time-scale faster than several minutes. In other instances, within the same cell, changes took place over the course of tens of minutes. There are two possible mechanisms at work, cytoskeletal structures could extend or shorten in the cortical plane or they could move out of or into the plane from a position deeper in the cell. We do not see any obvious effects on ABM or IBM remodeling that are tip induced. When we vary the time interval between images the rate of movement (in IBM remodeling) remains constant, suggesting that the cell is not responding to the repeated imaging. However, we cannot exclude the possibility that the initial contact between tip and cell initiates some of the events described here, in particular since endothelial cells sense and respond to mechanical forces [2,16].

4. Discussion

The organization and dynamics of the cortical cytoskeleton in BPAECs reported here have a number of implications. To begin with, the modes of cortical remodeling seen here may be important for regulating mechanically induced signaling. Vascular endothelial cells respond to external mechanical stimuli through a variety of mechanisms, including mechanical coupling via integrins to the cytoskeleton [2,16]. For IBM remodeling, the integrin to cytoskeleton connection can remain intact as the mesh elements move. Thus, the position of integrins could be controlled by IBM type movement of the cytoskeleton, and the integrin would remain mechanically coupled to the cellular cytoskeleton. However, for ABM remodeling, integrin–cytoskeleton interactions would have to be altered. In particular, when a cytoskeletal filament leaves the cortex any integrin mediated connections to the extracellular environment would be lost, which in turn would disconnect those integrins from the signaling pathway. There is biochemical evidence that the Src tyrosine kinase can modulate

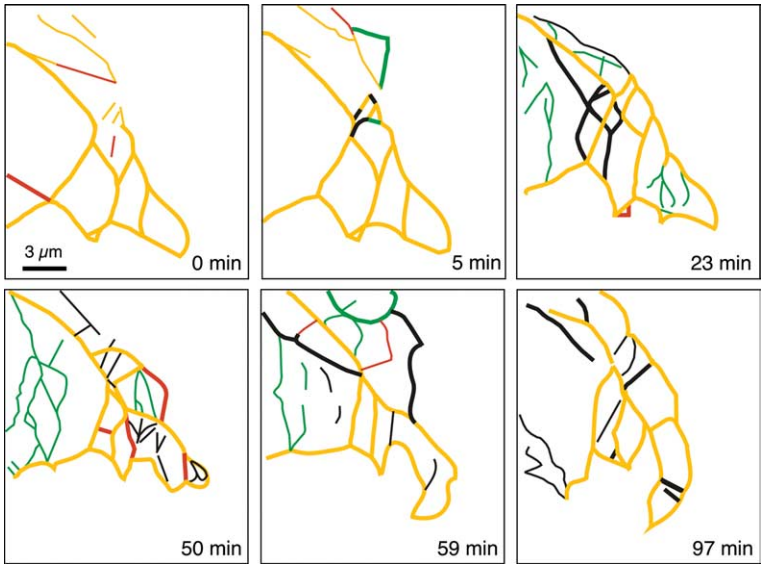

Fig. 4. ABM remodeling of the cortical mesh. Hand traces of coarse mesh boundaries from Fig. 2 that show ABM type remodeling. In this mode of remodeling existing boundaries disappear from cortex, while new boundaries appear. Here, changes are color coded: red filaments will disappear in the next frame, black filaments were not in the previous frame, green filaments were not in the previous frame and will disappear in the next frame, and orange filaments show no change between consecutive frames.

integrin–cytoskeleton association, thereby controlling cell traction forces [17]. ABM remodeling may be related to such a mechanism for regulating the interaction between cytoskeleton and the extracellular environment, or it may represent a distinct layer in the control system.

One limitation of the present study is that the analysis focuses on the coarse cytoskeletal mesh seen in the AFM images. These structures are sufficiently stiff to produce good contrast, while the finer mesh is difficult or impossible to fully trace in sequential images. However, the fine mesh appears to run over the coarse mesh in some places and under in others, and thus the two meshes may be intertwined [12]. If this is the case, the dynamics of the two are likely to be coupled. In the case of coupled dynamics, one can envision two possibilities: one where the fine mesh is relatively passive and the overall dynamics are dominated by the coarse mesh and another where the fine mesh has significant intrinsic dynamics which must be accounted for together with the coarse mesh dynamics. While we cannot at present account for the fine mesh dynamics, an understanding of the coarse mesh dynamics is important in either case.

The cortical cytoskeleton has also been proposed to play a role in membrane domain formation; in the so-called anchored-picket fence model, a cortical mesh restricts movement of proteins and lipids by confining their cytoplasmic domains to a cytoskeletal compartment [6,18]. Diffusion measurements in a variety of cells suggest a characteristic domain size of 30–300 nm [19,20]. This is on the same order as the fine mesh seen here, but substantially smaller than the coarse mesh. The small compartments have also been referred to as corrals, and it has been noted that such corrals might be static or dynamic [21]. One interpretation of our data is that IBM remodeling corresponds to static corrals, where molecules would tend to remain confined. Although a notable difference is that while the boundaries of corrals in IBM remain intact (i.e., are "static"), they also move and change shape. Escape from such confinement could involve membrane fluctuations or some change in the interaction of the confined molecule with the corral. ABM dynamics on the other hand would be conceptually similar to the proposed "dynamic corral" model for controlling intercompartmental movement of membrane molecules, where boundaries of existing corrals are lost and new ones are formed over time [21]. Thus, the results presented here suggest that the static corrals may actually move, and that static and dynamic corrals may co-exist. With respect to this interpretation, we note that the measurements presented here are on a much longer time scale than the single particle tracking experiments that form the primary basis for the picket fence model. However, if indeed the fine and coarse meshes are intertwined, then the fine mesh dynamics will depend at least in part on the coarse mesh dynamics.

The AFM studies initiated here provide the ability to examine structurally and functionally important aspects of cytoskeletal dynamics in the cortex of living cells. However, AFM technology is still rapidly evolving, particularly in biology, and much work remains to be done in developing methods for optimal AFM imaging of living cells. This suggests that further insight, including direct visualization of fine mesh dynamics, is likely forthcoming. In addition, integrating AFM experiments with other types of approaches will likely prove to be very useful in understanding cells of the vascular endothelium.

Acknowledgments: We thank Dr. Michael Edidin, Dr. Joseph Garcia, Dr. Susan Craig and Dr. Douglas Robinson for helpful discussions. We are also very grateful to Marlene Carlyle and Digital Instruments/Veeco for loan of the BioScope AFM used in the work described here. This work was supported in part by a grant from the National Institutes of Health (HL076241).

References

[1] Malek, A.M. and Izumo, S. (1996) Mechanism of endothelial cell shape change and cytoskeletal remodeling in response to fluid shear stress. J. Cell Sci. 109, 713–726.
[2] Ingber, D.E. (2002) Mechanical signaling and the cellular response to extracellular matrix in angiogenesis and cardiovascular physiology. Circ. Res. 91, 877–887.
[3] Davies, P.F. (1995) Flow-mediated endothelial mechanotransduction. Physiol. Rev. 75, 519–560.
[4] Barbee, K.A., Mundel, T., Lal, R. and Davies, P.F. (1995) Subcellular distribution of shear stress at the surface of flow-aligned and nonaligned endothelial monolayers. Am. J. Physiol. 268, H1765–H1772.
[5] Saxton, M.J. and Jacobson, K. (1997) Single-particle tracking: applications to membrane dynamics. Annu. Rev. Biophys. Biomol. Struct. 26, 373–399.
[6] Kusumi, A., Suzuki, K. and Koyasako, K. (1999) Mobility and cytoskeletal interactions of cell adhesion receptors. Curr. Opin. Cell. Biol. 11, 582–590.
[7] Izumi, T., Shibata, Y. and Yamamoto, T. (1991) Quick-freeze, deep-etch studies of endothelial components, with special reference to cytoskeletons and vesicle structures. J. Electron Microsc. Technol. 19, 316–326.
[8] Heuser, J.E. and Kirschner, M.W. (1980) Filament organization revealed in platinum replicas of freeze-dried cytoskeletons. J. Cell Biol. 86, 212–234.
[9] Galbraith, C.G., Skalak, R. and Chien, S. (1998) Shear stress induces spatial reorganization of the endothelial cell cytoskeleton. Cell Motil. Cytoskeleton 40, 317–330.
[10] Henderson, E., Haydon, P.G. and Sakaguchi, D.S. (1992) Actin filament dynamics in living glial cells imaged by atomic force microscopy. Science 257, 1944–1946.
[11] Hofmann, U.G., Rotsch, C., Parak, W.J. and Radmacher, M. (1997) Investigating the cytoskeleton of chicken cardiocytes with the atomic force microscope. J. Struct. Biol. 119, 84–91.
[12] Pesen, D., Hoh, J.H. Micromechanical architecture of the endothelial cell cortex. Biophys. J. In press.
[13] Jeffery, T.K. and Wanstall, J.C. (2001) Pulmonary vascular remodeling: a target for therapeutic intervention in pulmonary hypertension. Pharmacol. Ther. 92, 1–20.
[14] Dudek, S.M. and Garcia, J.G. (2001) Cytoskeletal regulation of pulmonary vascular permeability. J. Appl. Physiol. 91, 1487–1500.
[15] Helmke, B.P., Goldman, R.D. and Davies, P.F. (2000) Rapid displacement of vimentin intermediate filaments in living endothelial cells exposed to flow. Circ. Res. 86, 745–752.
[16] Helmke, B.P. and Davies, P.F. (2002) The cytoskeleton under external fluid mechanical forces: hemodynamic forces acting on the endothelium. Ann. Biomed. Eng. 30, 284–296.
[17] Felsenfeld, D.P., Schwartzberg, P.L., Venegas, A., Tse, R. and Sheetz, M.P. (1999) Selective regulation of integrin–cytoskeleton interactions by the tyrosine kinase Src. Nat. Cell Biol. 1, 200–206.
[18] Nakada, C., Ritchie, K., Oba, Y., Nakamura, M., Hotta, Y., Iino, R., Kasai, R.S., Yamaguchi, K., Fujiwara, T. and Kusumi, A. (2003) Accumulation of anchored proteins forms membrane diffusion barriers during neuronal polarization. Nat. Cell Biol. 2003 (5), 626–632.
[19] Kusumi, A., Sako, Y. and Yamamoto, M. (1993) Confined lateral diffusion of membrane receptors as studied by single particle tracking (nanovid microscopy). Effects of calcium-induced differentiation in cultured epithelial cells. Biophys. J. 65, 2021–2040.
[20] Ritchie, K., Iino, R., Fujiwara, T., Murase, K. and Kusumi, A. (2003) The fence and picket structure of the plasma membrane of live cells as revealed by single molecule techniques. Mol. Membr. Biol. 20, 13–18.
[21] Leitner, D.M., Brown, F.L. and Wilson, K.R. (2000) Regulation of protein mobility in cell membranes: a dynamic corral model. Biophys. J. 78, 125–135.